PLANAR TRANSFORMER FOR ENERGY HARVESTING APPLICATIONS

Yelda VELI[1], Alexandru M. MOREGA[1], Lucian PÎSLARU–DĂNESCU[2], Mihaela MOREGA[1]

The paper is concerned with the numerical analysis of two designs of planar, miniature, flyback transformer (FBT) powered up by a pulse width modulated (PWM) voltage supply at high frequency. The first model uses a nonmagnetic medium for a part of the magnetic circuit, whereas the second design uses a magnetic nanofluid (MNF). The provided air gap in the central column of the ferrite core, which has the role of enhancing the stored magnetic energy, is varied. The thermal analysis accompanies this study.

Keywords: flyback transformer, planar transformer, energy harvesting, conversion, numerical simulation, thermal stability, magnetic nanofluid

1. Introduction

The emerging development of energy harvesting low power applications necessitates creating new solutions for the conversion stage of such devices. A vital component of this stage is the flyback transformer (FBT), which temporarily stores and then delivers magnetic energy.

Depending on how much energy is to be delivered to the load, two main operation modes may occur, the *continuous conduction mode* (CCM) and the *discontinuous conduction mode* (DCM), which is analyzed in this paper [1,2].

Magnetic nanofluids are widely used in various applications for cooling purposes, magnetic particle delivery, coupling element, etc. [4-8]. The simplified device introduced in [1,2] and analyzed in this paper is a 1:1 planar FBT powered by a high-frequency PWM voltage supply provided with four circular, cylindrical disk-type coils, electrical coupled two by two in series, forming the primary, respectively the secondary winding. This study is concerned with evaluating the effect of replacing the nonmagnetic spacer that is positioned between the primary and secondary windings with a magnetic nanofluid (MNF) with a colloidal suspension of magnetic nanoparticles of 500 Gs and UTR40 transformer oil as the carrier, *e.g.*, [1]. The central column of the FBT, shown in Fig.2, is provided with

[1] Faculty of Electrical Engineering, the University POLITEHNICA of Bucharest, Romania, e-mail: yelda.veli@yahoo.com, amm@iem.pub.ro, mihaela@iem.pub.ro
[2] National Institute for Research and Development in Electrical Engineering ICPE-CA, Bucharest, Romania, e-mail: lucian.pislaru@icpe-ca.ro

an air gap [1] to enhance energy storage since only a small amount may be stored in a low reluctance circuit.

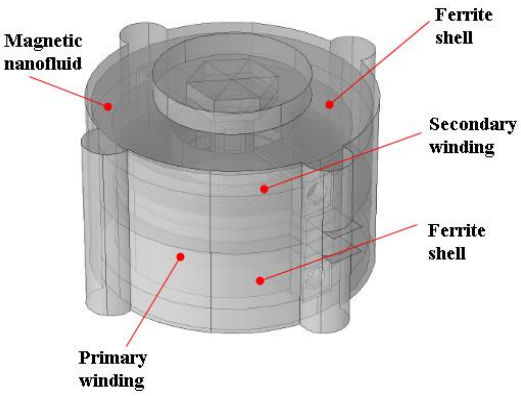

Fig. 1. The transformer in [2] with spiral shell windings.

To better view the components and the material used in designing the device, an axial crosscut view is provided in Fig. 2, for a simplified version of the device shown in Fig. 1.

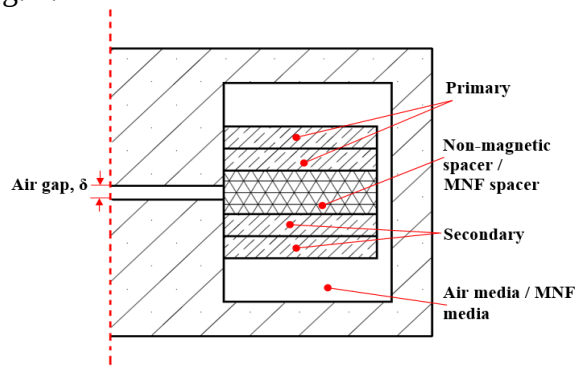

Fig. 2. Crosscut view of the device [1].

The spacer between the windings and the surrounding space is in one case (design A) made from a nonmagnetic material, FR4 and air, and in the second case (design B) from a highly magnetic one, the MNF. The windings have 20 turns each. Quasi-stationary working conditions are assumed. The electromagnetic field is analyzed for both designs and different sizes of the airgap, δ. A thermal stability analysis is also performed.

2. The mathematical model

The magnetic field inside design (A) is described assuming axial symmetry:

$$\sigma\frac{\partial \mathbf{A}}{\partial t}+\nabla\times\left(\mu_0^{-1}\mu_r^{-1}\nabla\times\mathbf{A}\right)=\mathbf{J}^e, \tag{1}$$

where **A** [T·m] is the magnetic vector potential, μ_0 is the permeability of the free space, μ_r is the relative permeability, and $\mathbf{J}_e$ [A/m^2] is the external electric current density inside the coils windings.

The magnetic field for design (B), filled with MNF, is described by:

$$\sigma\frac{\partial \mathbf{A}}{\partial t}+\nabla\times\left(\mu_0^{-1}\mu_r^{-1}\nabla\times\mathbf{A}-\mathbf{M}\right)=0, \tag{2}$$

where **M** [A/m] is the magnetization (isotropic). The working conditions are such that the MNF behaves as a linear magnetic medium for which the isotropic, linear *M-H* relation:

$$M=\alpha\arctan(\beta H)\approx\alpha\beta H=\chi H, \tag{3}$$

holds. Here χ is the magnetic susceptivity, and α = 7.668·10^{-8} [A/m] and β = 6.78·10^{-4} [m/A] are empiric constants that provide for the best fit of the experimental curve [1,2].

The boundary conditions (BCs) that close the mathematical model (1)-(3) are magnetic insulation for both magnetic and electric fields, except for the coils' terminals where circuit-type BCs are set to model the PWM source and the load, respectively. The equivalent electrical circuit is shown in Fig. 3 (adapted after [1]).

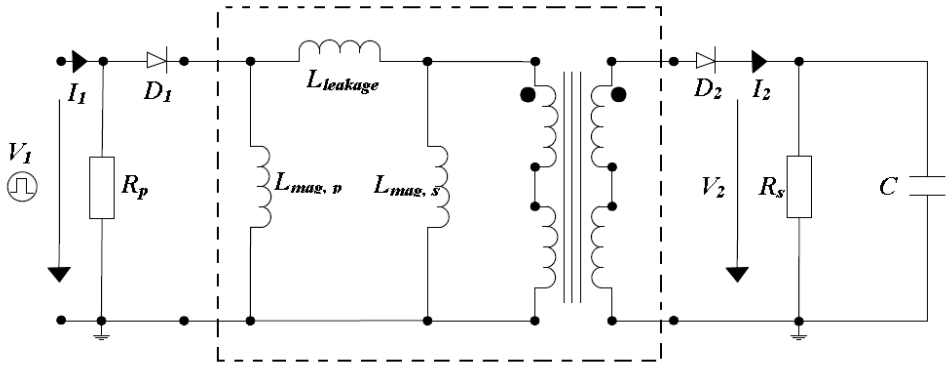

Fig. 3. The electrical circuit for the FBT with a PWM voltage supply at 10kHz, with RC load (C = 0.003 mF, R = 1 Ω).

The stationary form of the energy balance describes the thermal field:

$$\nabla\cdot\left(k\nabla T\right)+Q=0, \tag{4}$$

where k [W·m^{-1}·K^{-1}] is the thermal conductivity, T [K] is the temperature, Q [W/m^3] is the heat source (Joule losses inside the windings). The BCs are natural convection

for the side and top walls (h = 2 W·m^{-2}·K^{-1}), and thermal insulation for the base.

3. Results

We present numerical simulation results for design (A) with nonmagnetic material spacer and air and design (B) with MNF. The PWM voltage source provides for 6 V at 10 kHz, with a duty cycle $D = t_{on}/T = 0.3$, Fig. 4..

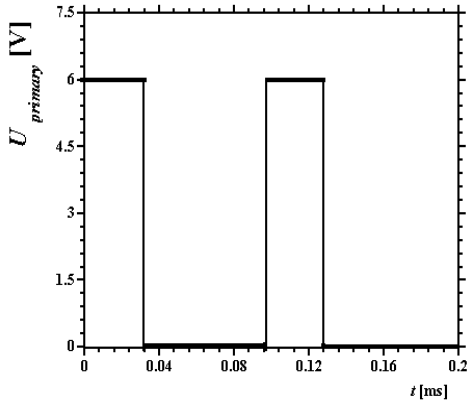

Fig. 4. The PWM voltage supply, at 6 V and 10 kHz, with a duty cycle of $D = t_{on}/T = 0.3$.

Figs. 5, 6 show the magnetic field distribution for different *on* and *off* times (Fig. 4) for the δ = 1 mm case.

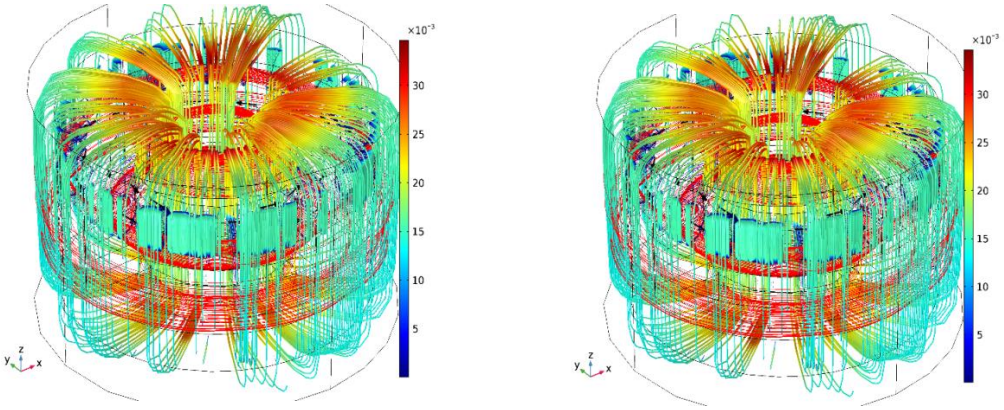

a. Design (A) – FBT with FR4 and air. b. Design (B) – FBT with MNF.

Fig. 5. Magnetic flux density at t = 0.14 ms, the primary is *on*, secondary is *off* for δ = 1 mm, C = 0.003 mF, and R = 1 Ω. Values are in Tesla.

The magnetic flux density decreases when increasing the air gap size, δ. The design (B) (with MNF) shows off lower values of magnetic flux density in comparison with design (A). Due to the high-frequency operation mode, the displacement current density contributes to the magnetic field for (horizontal,

circular field lines colored in red in Figs. 5,6).

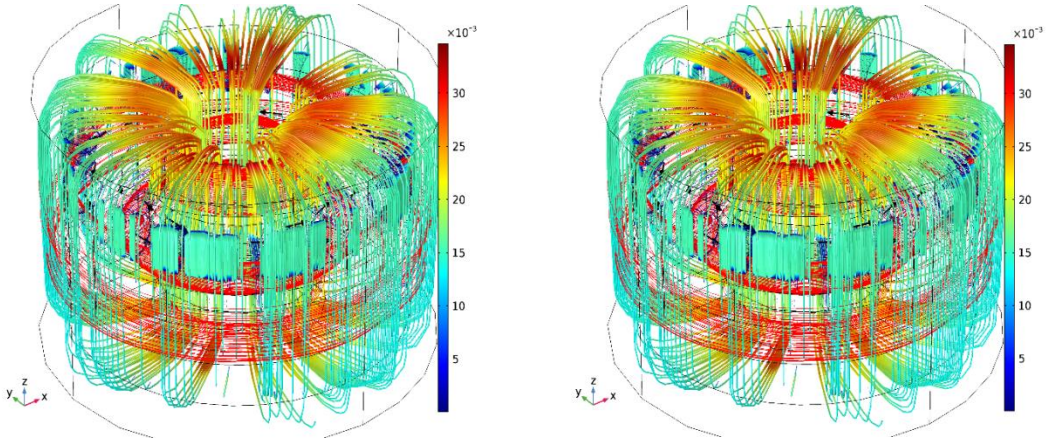

a. Design (A) – FBT with FR4 and air. b. Design (B) – FBT with MNF.

Fig. 6. Magnetic flux density at t = 0.18 ms, the primary is *on*, secondary is *off* for δ = 1 mm, C = 0.003 mF, and R = 1 Ω. Values are in Tesla.

Figs. 7 and 8 present the primary and secondary electric currents over a period for both designs and different sizes of δ.

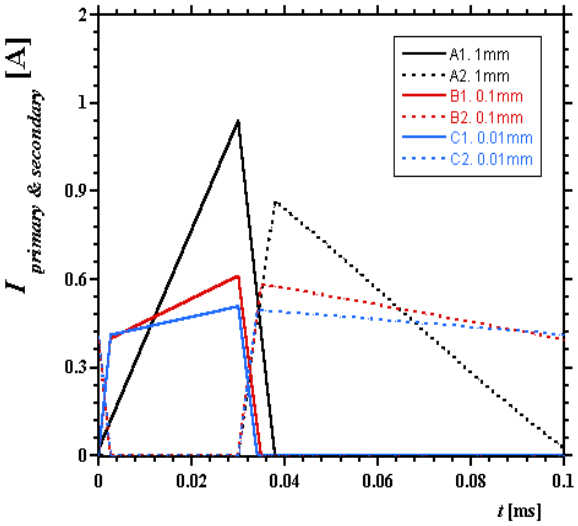

Fig. 7. Primary (continuous lines) and secondary currents (dotted lines) for δ = 1 mm, 0.1 mm, and 0.01 mm, for design (A).

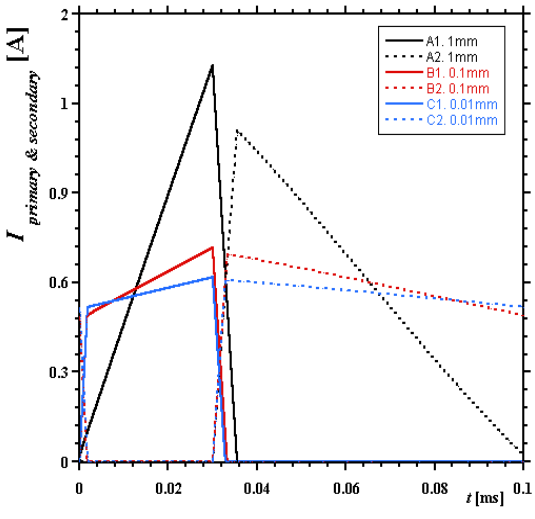

Fig. 8. Primary (continuous lines) and secondary currents (dotted lines) for δ = 1 mm, 0.1 mm, and 0.01 mm, for design (B).

Design (B) with the MNF presents higher primary current values versus the secondary current. The decrease of δ results in the reduction of the current values. Their shapes also change from triangular to trapezoidal. The maximum instantaneous value of the magnetic energy density inside the air gap inside the

central column of the ferrite core is found for δ = 0.23 mm, Fig. 11. The stored magnetic energy is computed by integrating the magnetic energy density over the air gap volume at the end of the "on" time sequence.

The average electric current values for primary and secondary winding for both designs and different air gap sizes are shown in Fig. 12. The minimum values are identifiable around δ = 0.25 mm. As these results suggest, δ may be an optimization design parameter.

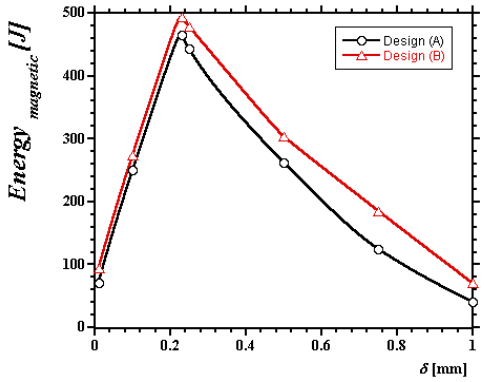

Fig. 11. Magnetic energy for different δ sizes.

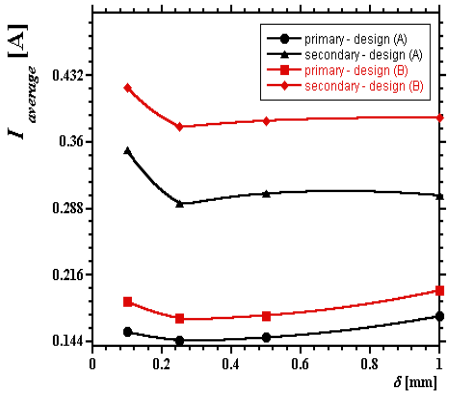

Fig. 12. Average current values for different δ sizes.

We may infer then that the MNF contributes to enhancing the energy storage capacity inside the air gap. The electric power of the capacitor and the load resistor is presented in more detail in [1].

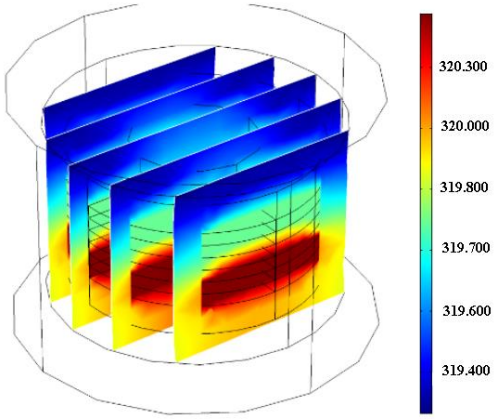

a. Design (A) – FBT with FR4 and air.

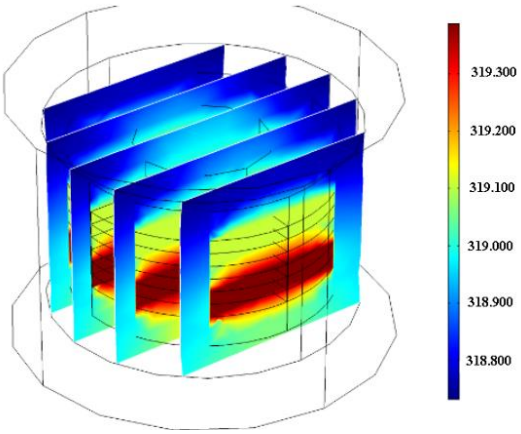

b. Design (B) – FBT with MNF.

Fig. 13. The temperature distribution when the primary is on and secondary is off. Values are in Kelvin.

In what concerns the heat transfer inside the transformer, the electric and magnetic field time scales are much smaller than the heat transfer time scale. For this reason, we consider the Joule losses inside the coils as the heat source, and we use the effective (RMS) value of the primary and secondary currents for both

design cases. The simulation results obtained through solving the mathematical model (4) for the temperature distribution are presented in Fig. 13 for $\delta = 0.25$ mm.

The material properties can explain why the heating up of the secondary winding appears to be much worse than that for the primary winding, as the FR4 spacer and the air domain presents a smaller thermal conductivity. The difference between the heating of the primary and secondary windings is at the limit of a degree.

The usage of the MNF material is convenient since it leads to lower temperature values. Hence MNF design (B) is somewhat cooler than design (A). However, it should be noticed that the effective electric current values (hence Joule heating) for the design (B) device are higher than for design (A).

4. Conclusions

This study is concerned with the mathematical modeling and numerical simulation results for two designs of flyback transformer (FBT): design (A) with nonmagnetic FR4 spacer and air and design (B), FBT with MNF media, which are powered up by a PWM voltage supply at 6V and 10 kHz, with a duty cycle of $D = t_{on}/T = 0.3$ and an air gap inside the central column of the ferrite core. The thickness of the column air gap is changed from 1 mm to 0.01 mm. The numerical simulation results for the electromagnetic field problem pinpoint an optimal air gap size, where the device's magnetic energy and storing capacity are at maximum. The analysis of the two designs made it possible to conclude the proper magnetic circuit design that may improve the primary-to-secondary energy switching performance of the FBT device.

The numerical simulation results show the advantage of using the MNF as compared to nonmagnetic FR4. The MNF design (B) shows off better magnetic coupling between the windings and better magnetic energy storage capacity. The stored magnetic energy inside the air gap at $\delta = 0.23$ mm is much higher for design (B) than design (A). The design (B) also exhibits a good temperature distribution, being somewhat cooler than the design (A) device. This finding is important because both designs are suitable to work in harsh environments for a long time.

Acknowledgement

The numerical simulations were conducted in the Laboratory of Multiphysics Modeling at UPB, as a follow up of the research grant UEFISCDI, PNCDI II Programme – Joint Applied Research Projects, Romania, research grant no. 63/2014 “Environment energy harvesting hybrid system by photovoltaic and piezoelectric conversion, DC/DC transformation with MEMS integration and adaptive storage”.

REFERENCES

[1]. *Yelda Veli, A.M. Morega, L. Pîslaru – Dănescu, M. Morega*, „Numerical modeling of a flyback transformer with different magnetic media, for micro-power controllers", ICATE 2018, Craiova, Romania, Oct. 2018.

[2]. *J.B. Dumitru, A.M. Morega, L. Pislaru-Danescu, M. Morega*, "High-frequency miniature planar transformer for energy harvesting applications", IEEE-EPE, 2016, Iasi, Romania.

[3]. *L. Pîslaru-Dănescu, A.M. Morega, G. Telipan, M. Morega, J.B. Dumitru, V. Marinescu*, "Magnetic nanofluid applications in electrical engineering", IEEE Trans. on Magnetics, 49, 11, 2013.

[4]. *T.H. Tsai, L.S. Kuo, P.H. Chen, D. Lee, C.T. Yang*, "Applications of ferro-nanofluid on a micro-transformer", Sensors, 2010, DOI 10.3390/s100908161.

[5]. *M.J. Prieto, A.M. Pernia, J.M. Lopera, J.A., F. Nuno*, "Design and analysis of thick-film integrated inductors for power converters", IEEE Transactions on Industry Applications, 38, 2, 2002.

[6]. *C.I. Mocanu*, Theory of Electromagnetism, (in Romanian) Ed. Tehnica, Bucuresti, 1982.

[7]. *J.B. Dumitru, A.M. Morega, M. Morega, L. Pîslaru-Dănescu*, "Forced flow patterns in a miniature planar spiral transformer with ferrofluid core", INCAS Bulletin, 7, 4, pp. 85-94, 2015, Bucharest, Romania

[8]. *L. Kontorovych, V. Prykhodko*, "Use of mathematical models for design review of new under construction transformers and evaluating the condition of existing transformers in operation", Translab Ukraine, ZTZ Services Int. The USA.